Combined Hierarchical Wavelet-Coefficient Structures For Grayscale Image Compression

Dr. Anatoly.A. Boriskevich*, Dr.Viktar.Yu. Tsviatkou* & T.M. Al-juboori**

Received on:25/6/2009
Accepted on:3/12/2009

Abstract

A suitable algorithm suggested with wavelet compression for gray scale images based on one- and two-dimension combined hierarchical structure, in the sub-band which has been generated by the aid of several types of wavelet functions. It is shown that the using of combined based hierarchical structures allows us to reduce the calculations complexity of compression and decompression at constant values of compression coefficients.

أستخدام التركيب المعقد الشجيري لمعاملات المويجات في ضغط الصور ذات التدرج الرمادي

الخلاصة

تم اقتراح خوارزمية مناسبة باستخدام تقية ضغط المويجات (wavelet compression) في الصور ذات التدرج الرمادي لنطاق لحزمة الجانبية التي تم توليدها باستخدام انواع متعددة من الدوال المويجية .وقد تم أثبات بأنه عند أستخدام التركيب المعقد الشجيري المرتبي (combined based hierarchical structures)،فانه يمكننا من تقليل الخطأ في الحسابات المركبة عند عمليات الضغط وفتح الضغط لأقيام ثابتة في معاملات المعلومات المضغوطة

1. Introduction

Related to the intensive growth of the video traffic in networks of telecommunications, the major scientific and technical direction of development of techniques of transfer and distribution of the information are compression of video-data. The most effective algorithms are JPEG 2000, EZW, SPIHT, SPECK, etc. [1 - 11] which realize progressive compression of images in the field of wavelet-transformation. For achievement of high factors of compression in these algorithms, as a rule they are used the wavelet-factors calculated on the basis of biorthogonal wavelet-functions. It leads to the growth of computing complexity in comparison with a variant of use for compression of wavelet-functions Haar. The purpose of the present work is the estimation of efficiency of compression of half-tone pictures on the basis of the combined hierarchical structures in which wavelet-factors of various

* Telecomm. and Comp. Department, Belarusian state University/ Belarusian
** Ph.D Student, Belarusian state University/ Belarusian

levels are generated by means of different wavelet-functions.

2. Rational and integer-valued wavelet-transformations

The most effective approaches for lossy image compression and lossless based on the discrete wavelet transform coding, and tree structure of wavelet coefficients, formed in the frequency-spatial domain [1 - 4]. Discrete wavelet transform is implemented due to the using of two types of functional approximation (approximation and detailing), applied to discrete signals at different levels of decomposition. Approximation (scaling) functions have a smooth shape envelope. Detailing of the functions (wavelet function) characterize the local features of a different order in a discrete signal (gaps, jumps, etc.). One of the most important properties of wavelet functions is the spatial and frequency localization, quantitative measure that defines the spatial-frequency resolution. The lowest spatial-frequency resolution of wavelet functions are Haar (Fig. 1, a, b), and the largest - of biorthogonal wavelets. This is due to the use of biorthogonal wavelet functions 9.7 (Fig. 1, c, d) and 5.3 (Fig. 1, e, f) in the algorithm for JPEG 2000 image compression with losses and without losses. However, the wavelet transform based on biorthogonal wavelet functions requires significantly greater computational resources than the wavelet-transform based on Haar wavelet functions. Fig. 2 presents the basic scheme of one-dimensional sound and the direct integral wavelet transform based on Haar wavelet functions and biorthogonal wavelet functions, which are formed as a result of a low (L) and one high (H) wavelet coefficients.

Fig. 2, a and 2, b shows that the basic rational wavelet transform based on biorthogonal wavelet functions requires 9.7 to 4 times more multiplicative operations and 7 times more than double additive operations compared to the rational wavelet transform based on Haar wavelet function. From Fig. 2, c and 2, d it is shown that the basic integer-valued wavelet transform based on biorthogonal wavelet functions requires *5.3* to 2 times more than multiplicative and additive operations, compared with an integer-valued wavelet transform on Haar wavelet functions.

3. Hierarchical structure of the wavelet coefficients

In the frequency domain the wavelet transform can be represented as a bank of filters. Fig. 3 shows three-cascaded filter bank analysis and synthesis, carrying out a direct and inverse wavelet transform sound. multilevel discrete wavelet decomposition of signals obtained by recursive application of the low-frequency and high frequency filtering to the original values of the signal at the first iteration and the low wavelet coefficients at subsequent iterations. The direct and inverse wavelet transforms sound described by the following recurrent expression:

$$\begin{cases} W^{L}_{1\times\left(N/2^{r}\right)}(r) = f_{F}\left(W^{L}_{1\times\left(N/2^{r-1}\right)}(r-1), C^{L}_{1\times N_{L}}\right), \\ W^{H}_{1\times\left(N/2^{r}\right)}(r) = y_{F}\left(W^{L}_{1\times\left(N/2^{r-1}\right)}(r-1), C^{H}_{1\times N_{H}}\right), \end{cases} \quad \ldots\ldots(1)$$

$$W^{L}_{1\times\left(N/2^{r-1}\right)}(r-1)=$$
$$f_F^{-1}\left(W^{L}_{1\times\left(N/2^{r}\right)}(r),C^{H}_{1\times N_H}\right)+y_F^{-1}\left(W^{H}_{1\times\left(N/2^{r}\right)}(r),C^{L}_{1\times N_L}\right) \quad \ldots(2)$$

where f_F and y_F -direct rational wavelet transform using the approximation, and detailing the wavelet functions, f_F^{-1} and y_F^{-1} are inverse rational wavelet transform , $r=\overline{1,R}$ the number of wavelet decomposition, coinciding with the number of iterations ,R the number of levels of wavelet decomposition, $W^{L}_{1\times\left(N/2^{r}\right)}(r)$ and $W^{H}_{1\times\left(N/2^{r}\right)}$ are a matrices of low and high frequency wavelet coefficients at the level r of wavelet decomposition, $W^{L}_{1\times N}(0)=X_{1\times N}$ the matrix of wavelet coefficients of zero, coinciding with the values of discrete tone $X_{1\times N}$; N turned the number of discrete signal $C^{L}_{1\times N_L}$ and $C^{H}_{1\times N_H}$ the matrix of coefficients of the low-and high-frequency filter, and - the number of coefficients of the low-and high-frequency filters N_L and N_H are the direct and inverse integer-valued wavelet transform described by the following recursive expressions

$$\begin{cases} W^{L}_{1\times\left(N/2^{r}\right)}(r)=\phi_I\left(W^{L}_{1\times\left(N/2^{r-1}\right)}(r-1),W^{H}_{1\times\left(N/2^{r}\right)}(r)\right), \\ W^{H}_{1\times\left(N/2^{r}\right)}(r)=\psi_I\left(W^{L}_{1\times\left(N/2^{r-1}\right)}(r-1)\right), \end{cases} \quad \ldots..(3)$$

$$W^{L}_{1\times\left(\frac{N}{2^{r-1}}\right)}(r-1)= \begin{cases} f_I^{-1}\left(W^{L}_{1\times\left(\frac{N}{2^{r}}\right)}(r),W^{H}_{1\times\left(\frac{N}{2^{r}}\right)}(r)\right) \\ \text{For even coefficients}, \\ y_I^{-1}\left(W^{L}_{1\times\left(\frac{N}{2^{r-1}}\right)}(r-1),W^{H}_{1\times\left(\frac{N}{2^{r}}\right)}(r)\right) \\ \text{For odd coefficients}, \end{cases} \quad \ldots..(4)$$

Where f_I and y_I direct integral wavelet transform using the approximation, and detailing the wavelet functions, f_I^{-1} and y_I^{-1} are the backward integer-valued wavelet transform.

The tree structure is obtained by combining the wavelet coefficients at all levels of transformation and accession to the low-frequency coefficients of the last level (Fig. 4).

One dimensional tree structure includes a degenerate tree of L (approximation ratio) and the tree H (detailing the factors). When building two tree structures using a one-dimensional wavelet transform applied to the first row and then two columns to the matrix of input data or the wavelet coefficients. In doing so, formed four sub-band coefficients (LL - approximation ratio; HL, HH, LH - detailing coefficients). Similarly, we construct three-dimensional tree structure, which includes eight sub-bands. The number of wavelet coefficients in the tree structure is equal to the number of discrete and dimension (the dimension of the space) tree

structure of wavelet coefficients coincides with the dimension turned the discrete signal.

4. Combined treelike structure of the wavelet coefficients

In image compression algorithms, already used homogeneous hierarchal structure of the wavelet coefficients generated using the wavelet functions of the same type, as a rule, biorthogonal. To reduce the computational complexity of compression and decompression of images with lossy and lossless proposed algorithm combined forming trees in which the coefficients of the different levels of decomposition are formed by using different wavelet functions. The algorithm is based on the following terms

$$\begin{cases} W^{L}_{1\times\left(N/2^{r}\right)}(r)=f_F\left(W^{L}_{1\times\left(N/2^{r-1}\right)}(r-1),C^{L}_{1\times N_L}(r)\right), \\ W^{H}_{1\times\left(N/2^{r}\right)}(r)=y_F\left(W^{L}_{1\times\left(N/2^{r-1}\right)}(r-1),C^{H}_{1\times N_H}(r)\right), \end{cases} \quad \text{.....(5)}$$

$$W^{L}_{1\times\left(N/2^{r-1}\right)}(r-1)=f_F^{-1}\left(W^{L}_{1\times\left(N/2^{r}\right)}(r),C^{H}_{1\times N_H}(r)\right)+ +y_F^{-1}\left(W^{H}_{1\times\left(N/2^{r}\right)}(r),C^{L}_{1\times N_L}(r)\right) \quad \text{.... (6)}$$

$$\begin{cases} W^{L}_{1\times\left(N/2^{r}\right)}(r)=\phi_I(r)\left(W^{L}_{1\times\left(N/2^{r-1}\right)}(r-1),W^{H}_{1\times\left(N/2^{r}\right)}(r)\right), \\ W^{H}_{1\times\left(N/2^{r}\right)}(r)=\psi_I(r)\left(W^{L}_{1\times\left(N/2^{r-1}\right)}(r-1)\right), \end{cases} \quad \text{....(7)}$$

$$W^{L}_{1\times\left(N/2^{r-1}\right)}(r-1)= \begin{cases} f_I^{-1}(r)\left(W^{L}_{1\times\left(N/2^{r}\right)}(r),W^{H}_{1\times\left(N/2^{r}\right)}(r)\right) \\ \text{For even coefficients,} \\ y_I^{-1}(r)\left(W^{L}_{1\times\left(N/2^{r-1}\right)}(r-1),W^{H}_{1\times\left(N/2^{r}\right)}(r)\right) \\ \text{For odd coefficients,} \end{cases} \quad \text{.....(8)}$$

Where $C^{L}_{1\times N_L}(r)$ and $C^{H}_{1\times N_H}(r)$ the matrix of coefficients of the low-and high-frequency filters at the level r of decomposition $f_I(r)$, $y_I(r)$, $f_I^{-1}(r)$, $y_I^{-1}(r)$ forward and backward integer-valued wavelet transform at the level of decomposition.

At lower levels of wavelet decomposition is proposed to use biorthogonal wavelet functions that provide high spatial-frequency resolution and a compact presentation of information on small parts of images, but on top - Haar wavelet function for high spatial resolution and a compact representation of the major details of the prevailing in the low-frequency area of the upper levels of wavelet decomposition. This reduces the computational complexity of constructing combined trees of wavelet coefficients. For one-dimensional signal consisting of N discrete Multiplicative $g_M(R)$ and additive $g^1_A(r)$ computational complexity of constructing tree structures for R iterations are determined based on the number of multiplicative $g^1_M(r)$

and additive $g_A^1(r)$ operations, realizing the basic wavelet transform at each iteration r for one low and one high-frequency wavelet coefficients, using the following Expressions :

$$g_M(R) = \sum_{r=1}^{R}\left(\frac{N}{2^{r-1}}\cdot g_M^1(r)\right), \quad \text{.....(9)}$$

$$g_A(R) = \sum_{r=1}^{R}\left(\frac{N}{2^{r-1}}\cdot g_A^1(r)\right). \quad \text{.....(10)}$$

Table. 1 presents the quantitative characteristics of computational complexity of constructing one 18-level similar and combined trees of rational and integer-valued wavelet coefficients for test images of half-size 512×512 pixels, in the form of one-dimensional matrices 1×262144 . In the table used the following designations B^m and H^m - ***m***-level homogeneous treelike structure, using biorthogonal wavelet functions, 9.7 or 5.3 and Haar wavelet functions B^mH^n – $(m+n)$ combined treelike-tiered structure, using biorthogonal wavelet functions 9.7 and 5.3 at the lower m levels and Haar wavelet functions on the upper levels of ***n*** level $H^1B^mH^n$ – $(1+m+n)$ combined treelike structure, using Haar wavelet functions on the lower level, biorthogonal wavelet functions 9.7 and 5.3 m at the following levels and Haar wavelet functions on the upper level n . The ***F*** and ***I*** are subscripts, in the notation of tree structures to indicate the type of wavelet transform in rational or integer-valued.

From the table. 1 shows that the combined use of trees instead of a uniform tree-based biorthogonal wavelet functions reduces the multiplicative (additive) computational complexity in the 38-42% (43-48%) for the management of wavelet transform and 23-28% (25 -28%) for the integer-valued wavelet transform.

5. Valuation descriptions compactness combined trees

The effectiveness of combined trees can be evaluated by using algorithms of wavelet compression, lossy and lossless. In the tables 2 and 3 they are shown the characteristics of compression, lossy and lossless for standard grayscale test images «Lena» (low) and «Barbara» (a high) pixels in size, obtained through a one-dimensional version of the algorithm MECT [4] when using 18-level one-dimensional trees presented in the table. 1. The table shows that in comparison with similar trees derived from the biorthogonal wavelet functions, more complexity in simple combined treelike structures B^mH^n provide roughly the same, and sometimes higher peak signal-to-noise ratio and compression ratio. To compress grayscale images with the appropriate use of the combined losses of treelike structures $H_F^1B_F^3H_F^{14}$ that reduce computational complexity of the implementation of the wavelet decomposition of 28% compared with similar trees based on biorthogonal wavelet functions.

In the tables 4 and 5 it is shown that the characteristics of lossy

compression and lossless for the two versions of the algorithm MECT, obtained from the use of two 9-level tree structure. To compress grayscale images with a loss to use treelike structure of the combined type $B_F^1 H_F^8$ and $H_F^1 B_F^3 H_F^5$ when compression of 16 and 32 times using a tree structure $B_F^1 H_F^8$ for the combined restoration of the images are much better preserved fine details than with homogeneous structures H_F^9 and B_F^9. Using the tree structure $B_F^1 H_F^8$ provides a reduction of computational complexity of approximately 1.5 times compared with the tree structure B_F^9. When compression of 16 and 32 times, using a combined tree-structure on the reconstruction of the image block effect and no small parts saved about the same as when using a homogeneous structure $H_F^1 B_F^3 H_F^5$. The using of the tree structure provides a reduction of computational complexity of approximately 1.7-fold compared with the tree (a branch of hierarchal) structure B_F^9. Fig. 5 and 6 show the reconstructed test image «Lena» and «Barbara», compressed to 0.0625 bits per pixel (picture «Lena») and up to 0,125 bits per pixel (picture «Barbara») using two-dimensional algorithm MECT wavelet-based structures, indicated in Table. 4. From Fig. 5 and 6 shows that the use of wavelet structures, H_F^9, $B_F^1 H_F^8$, $B_F^2 H_F^7$ is affects the parameters of two-dimensional wavelet compression (on the reconstructed images clearly reveal a block effect). The wavelet structure $B_F^3 H_F^6$, $B_F^5 H_F^4$ and $H_F^1 B_F^3 H_F^5$ provides roughly the same quality of reconstruction of compressed images, wavelet-structure B_F^9, while reducing the computational complexity up to 1.7 times from (wavelet-structure $H_F^1 B_F^3 H_F^5$) .

6. Conclusions

The proposed algorithm has been used for formation of one-dimensional multi-layered combined trees of wavelet coefficients at the lower levels which the wavelet transform based on spatial-frequency localized biorthogonal wavelet functions, and on the upper level, a simple computational wavelet transform based on Haar wavelet functions. We show that in comparison with similar trees based on biorthogonal wavelet functions, the combined use of trees reduces the computational complexity of one-dimensional compression of grayscale images by approximately 40% for the management of wavelet transform and roughly 30% for integer-valued wavelet transformation while maintaining or improving peak signal-noise ratio and compression ratio. Using two-dimensional hierarchal structure of wavelet coefficients provides a reduction of computational complexity up to 1.7 times compared with homogeneous biorthogonal 9.7 wavelet structure with preservation of the quality of image reconstruction.

References

[1]. Joshi R.L. Comparison of multiple compression cycle performance for JPEG and JPEG 2000 , Proc. of the SPIE, San Diego,

CA, USA, July/August 2000. – Vol. 4115. P. 492-501.
[2]. Shapiro J.M. Embedded image coding using zerotress of wavelet coefficients , IEEE Trans. Signal Processing. – 1993. – No. 41. – P. 3445-3462.
[3]. Said A., Pearlman W.A. A new, fast, and efficient codec based on set partitioning in hierarchal trees , IEEE Trans. on Circuits and Systems for Video Technology. – 1996. – Vol. 6. – P. 243-250.
[4.] Boriskevich A.A., Tsviatkou V.YU. A method of scalable embedded image coding based on the hierarchical wavelet structure clustering , Doklady of the National Academy of Sciences of Belarus.– 2009. – Vol. 53, No. 3. – P. 42 – 48.
[5]. Islam A., Pearlman W.A. Set partitioned sub-block coding (speck) , ISO/IEC/JTC1/SC29, WG1 – No. 873. – 1998. – P. 312-326.
[6]. Chai B.-B., Vass J., Zhuang X. Significance-linked connected component analysis for wavelet image coding , IEEE Trans. Image Processing. – 1999. – Vol. 8, No. 6. – P. 774-784.
[7]. Servetto S., Ramchandran K., Orchard M.T. Wavelet based image coding via morphological prediction of significance , Proc. of IEEE International Conference on Image Processing. – 1995. – P. 530-533.
[8]. Cho S., Pearlman W.A. A full-featured, error resilient, scalable wavelet video codec based on the set partitioning in hierarchical trees (spiht) algorithm , IEEE Trans. on Circuits and Systems for Video Technology, March 2002.– Vol._12. – P. 157–171.
[9]. Lazzaroni F., Leonardi R., Signoroni A. High-Performance Embedded Morphological Wavelet Coding , IEEE Signal Processing Letters, Oct. 2003. – Vol. 10, No. 10. – P. 28-31.
[10]. Hwang W.-J., Wu C.-K., Li K.-J. Layered set partitioning in hierarchical tree for image coding , Signal Processing, 2002. – Vol. 82. – P. 149 – 156.
[11]. Cai C., Mitra S.K., Ding R. Smart wavelet image coding: X-tree approach , Signal Processing, 2002. – Vol. 82. P. 239 – 249.

Table (1) Computational complexity of forming one-dimensional trees complexity

Complexity Hierarchal structure	$g_M(18)$	$g_A(18)$		Complexity Hierarchal structure	$g_M(18)$	$g_A(18)$
B_F^{18}	**8388576**	**7340004**		B_I^{18}	**1048572**	**2097144**
H_F^{18}	**2097144**	**1048572**		H_I^{18}	**524286**	**1048572**
$B_F^1 H_F^{17}$	**5242872**	**4194300**		$B_I^1 H_I^{17}$	**786430**	**1572860**
$B_F^2 H_F^{16}$	**6815736**	**5767164**		$B_I^2 H_I^{16}$	**917502**	**1835004**
$B_F^3 H_F^{15}$	**7602168**	**6553596**		$B_I^3 H_I^{15}$	**983038**	**1966076**
$B_F^4 H_F^{14}$	**7995384**	**6946812**		$B_I^4 H_I^{14}$	**1015806**	**2031612**
$B_F^5 H_F^{13}$	**8191992**	**7143420**		$B_I^5 H_I^{13}$	**1032190**	**2064380**
$H_F^1 B_F^3 H_F^{14}$	**4849656**	**3801084**		$H_I^1 B_I^3 H_I^{14}$	**753662**	**1507324**

Table (2) Dependences of the peak signal-to-noise ratio (dB) of the compression ratio (bits per pixel) images «Lena» and «Barbara»

image	«Lena»				«Barbara»			
Compression Coefficient Hierarchal structure	2	1	0.5	0.25	2	1	0.5	0.25
B_F^{18}	**35.87**	**30.09**	**25.71**	**22.02**	**31.27**	**25.09**	**22.56**	**20.13**
H_F^{18}	**34.08**	**28.89**	**24.98**	**21.82**	**29.07**	**23.69**	**21.88**	**19.92**
$B_F^1 H_F^{17}$	**34.58**	**29.31**	**25.12**	**21.87**	**29.53**	**24.20**	**21.38**	**19.95**
$B_F^2 H_F^{16}$	**35.94**	**30.01**	**25.21**	**21.94**	**29.12**	**24.03**	**22.04**	**19.94**
$B_F^3 H_F^{15}$	**35.91**	**30.14**	**25.73**	**21.96**	**30.67**	**25.17**	**22.00**	**20.03**
$B_F^4 H_F^{14}$	**35.88**	**30.11**	**25.72**	**22.16**	**31.17**	**25.11**	**22.49**	**19.97**
$B_F^5 H_F^{13}$	**35.87**	**30.10**	**25.71**	**22.16**	**31.19**	**25.08**	**22.47**	**19.79**
$H_F^1 B_F^3 H_F^{14}$	**35.00**	**29.71**	**25.66**	**22.16**	**28.92**	**24.84**	**22.37**	**19.83**

Table (3) Compression ratio (times) Lossless of image «Lena» and «Barbara»

Hierarchal structure / Image	B_I^{18}	H_I^{18}	$B_I^1H_I^{17}$	$B_I^2H_I^{16}$	$B_I^3H_I^{15}$	$B_I^4H_I^{14}$	$B_I^5H_I^{13}$	$H_I^1B_I^3H_I^{14}$
«Lena»	**1.13**	**1.06**	**1.11**	**1.12**	**1.13**	**1.13**	**1.13**	**1.10**
«Barbara»	**1.04**	**0.99**	**1.02**	**1.03**	**1.04**	**1.04**	**1.04**	**1.01**

Table (4) Dependences of the peak signal-to-noise ratio (dB) of the compression ratio (bits per pixel) images ,Lena» and ,Barbara»

Image	,Lena»					,Barbara»				
Compression Coefficient Hierarchal structure	2	1	0.5	0.25	0.0625	2	1	0.5	0.25	0.125
B_F^9	**42.73**	**38.60**	**35.35**	**32.16**	**26.51**	**39.10**	**33.82**	**29.53**	**26.07**	**23.76**
H_F^9	**40.49**	**35.66**	**32.25**	**29.24**	**25.09**	**36.34**	**30.08**	**26.10**	**24.64**	**22.58**
$B_F^1H_F^8$	**42.04**	**37.38**	**33.89**	**30.43**	**25.29**	**38.50**	**33.28**	**28.17**	**25.46**	**22.90**
$B_F^2H_F^7$	**42.69**	**38.54**	**35.15**	**31.81**	**25.89**	**38.85**	**33.66**	**29.35**	**25.90**	**23.29**
$B_F^3H_F^6$	**42.74**	**38.60**	**35.33**	**32.02**	**26.42**	**39.08**	**33.80**	**29.52**	**26.06**	**23.54**
$B_F^4H_F^5$	**42.74**	**38.57**	**35.34**	**32.15**	**26.49**	**39.10**	**33.83**	**29.53**	**26.05**	**23.50**
$B_F^5H_F^4$	**42.74**	**38.61**	**35.37**	**31.99**	**26.41**	**39.10**	**33.83**	**29.53**	**26.05**	**23.75**
$H_F^1B_F^3H_F^5$	**40.94**	**36.34**	**32.98**	**30.30**	**26.31**	**37.45**	**30.91**	**26.80**	**25.11**	**23.57**

Table (5) Compression ratio (times) without loss of image «Lena» and «Barbara»

Hierarchal structure / Image	B_I^9	H_I^9	$B_I^1H_I^8$	$B_I^2H_I^7$	$B_I^3H_I^6$	$B_I^4H_I^5$	$B_I^5H_I^4$	$H_I^1B_I^3H_I^5$
«Lena»	**1.63**	**1.75**	**1.72**	**1.74**	**1.75**	**1.75**	**1.75**	**1.67**
«Barbara»	**1.44**	**1.56**	**1.54**	**1.55**	**1.56**	**1.56**	**1.56**	**1.46**

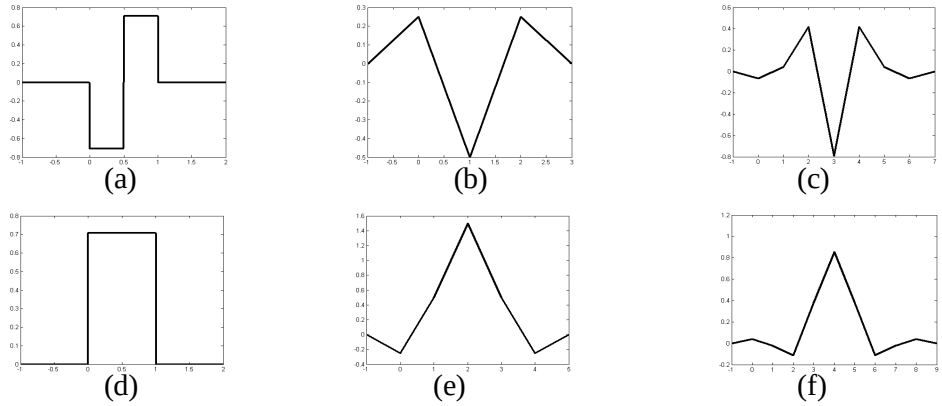

Figure (1) Wavelet-functions:
a and b are , Haar detailing (a) and approximation (b);
c,d- biorthogonal 5.3 detailing (a) and approximation (b);
e,f- biorthogonal 9.7 detailing (a) and approximation (b)

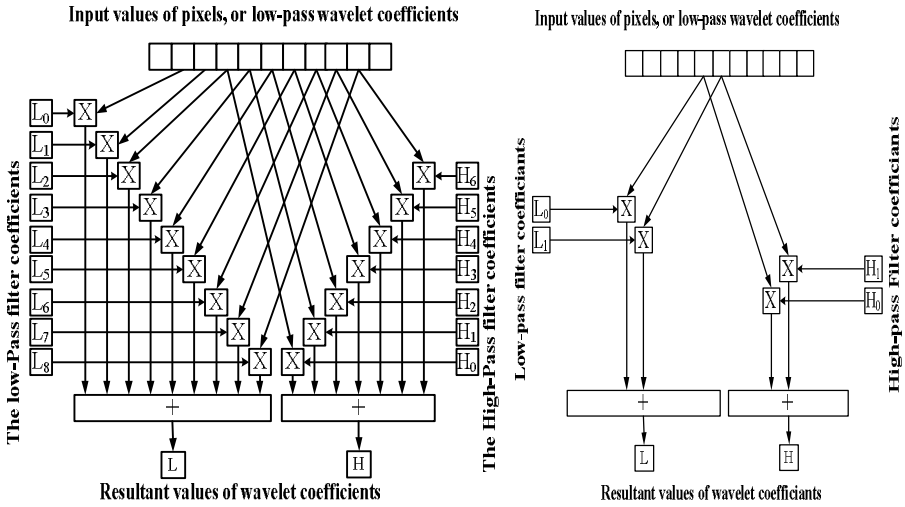

(a) (b)

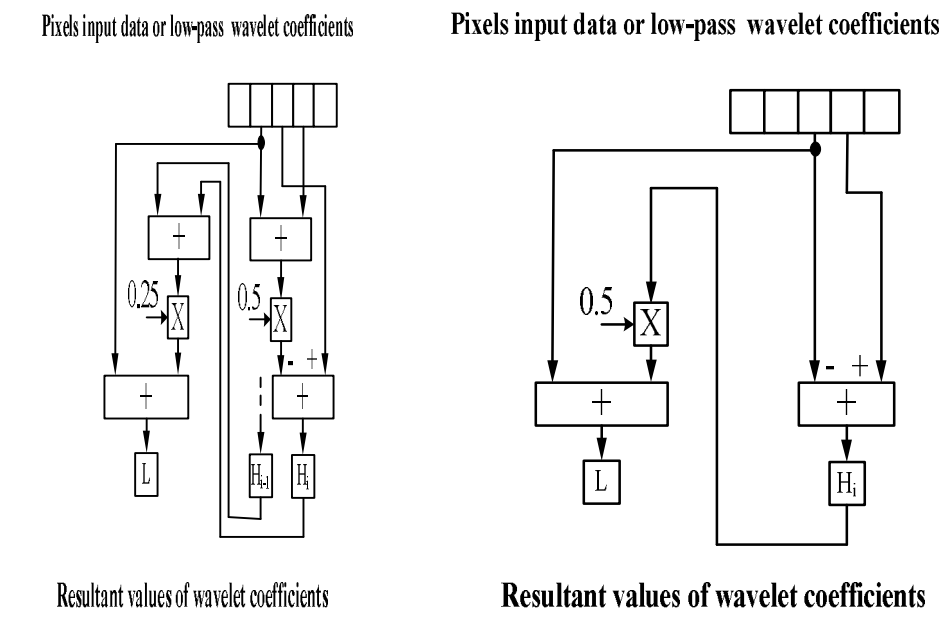

(c) (d)

Figure (2) The elementary one-dimensional wavelet transform:
a - rational wavelet transform based on biorthogonal wavelet functions, 9.7.
b - the rational wavelet transform based on Haar wavelet functions;
c - integer-valued wavelet transform based on biorthogonal wavelet functions, 5.3.
d- integer-valued wavelet transform based on Haar wavelet function.

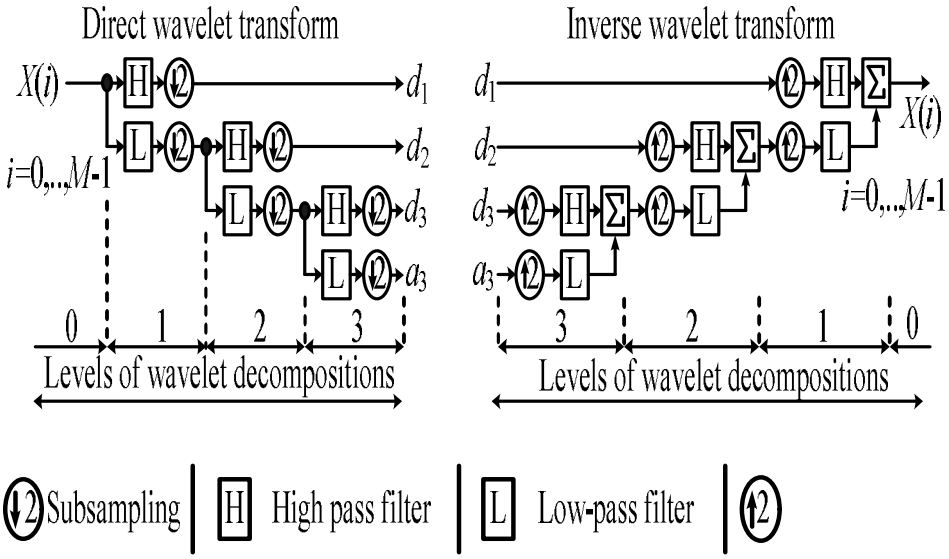

Figure (3) Block diagram of three-cascaded filter bank analysis and synthesis

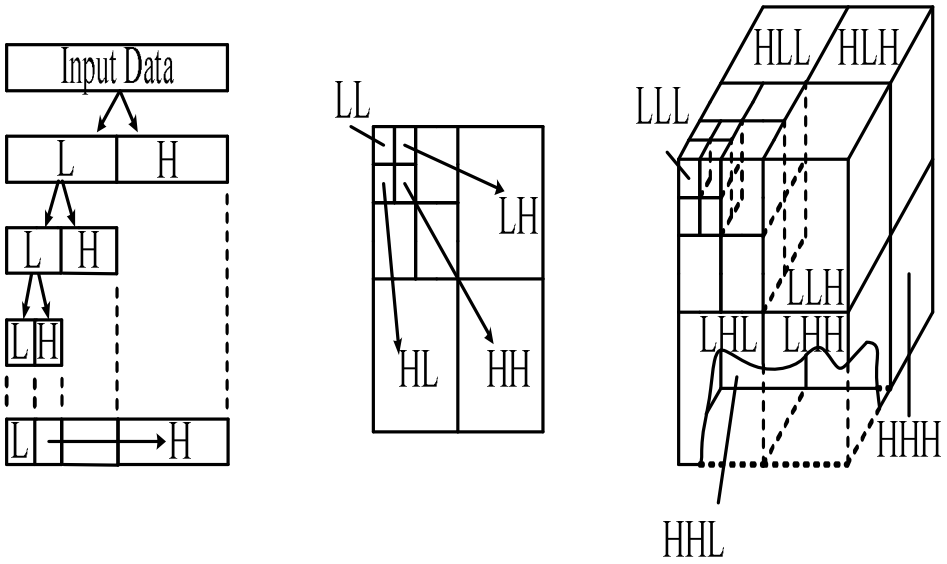

(a) (b) (c)

Figure (4) Hierarchal structure of the wavelet coefficients: a - one-dimensional; b - two-dimensional; c - three-dimensional

(a)

(b)

(c)

(d)

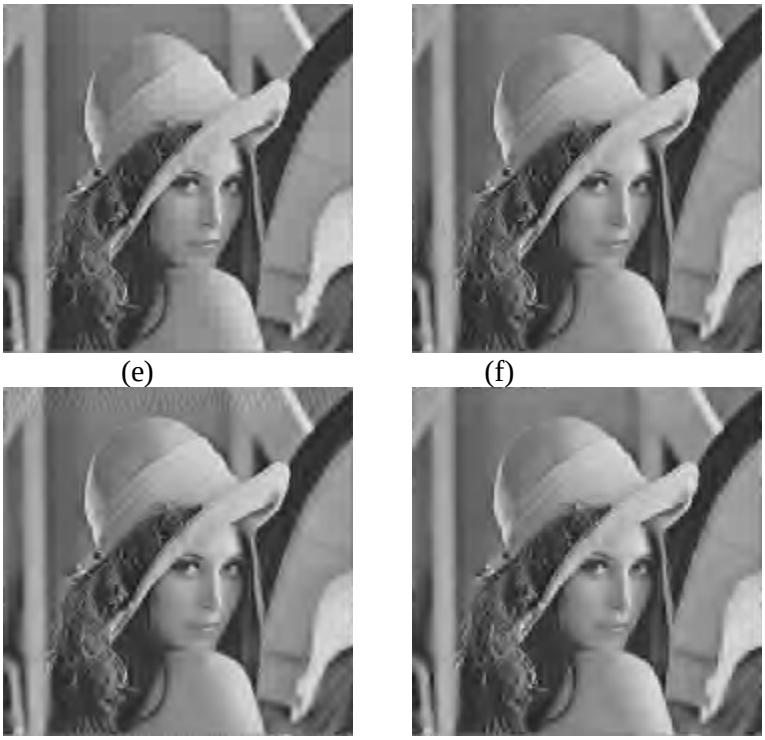

(e) (f)

(g) (h)

Figure (5) The restored version of the image «Lena», compressed to 0.0625 bpp using two-dimensional algorithm MECT bit wavelet-based structures:
a – B_F^9 **(26.51 dB); b –** H_F^9 **(25.09 dB); c –** $B_F^1 H_F^8$ **(25.29 dB); d –** $B_F^2 H_F^7$ **(25.89 dB); e –** $B_F^3 H_F^6$ **(26.42 dB); f –** $B_F^4 H_F^5$ **(26.49 dB); g –** $B_F^5 H_F^4$ **(26.41 dB); h –** $H_F^1 B_F^3 H_F^5$ (26.31 dB)

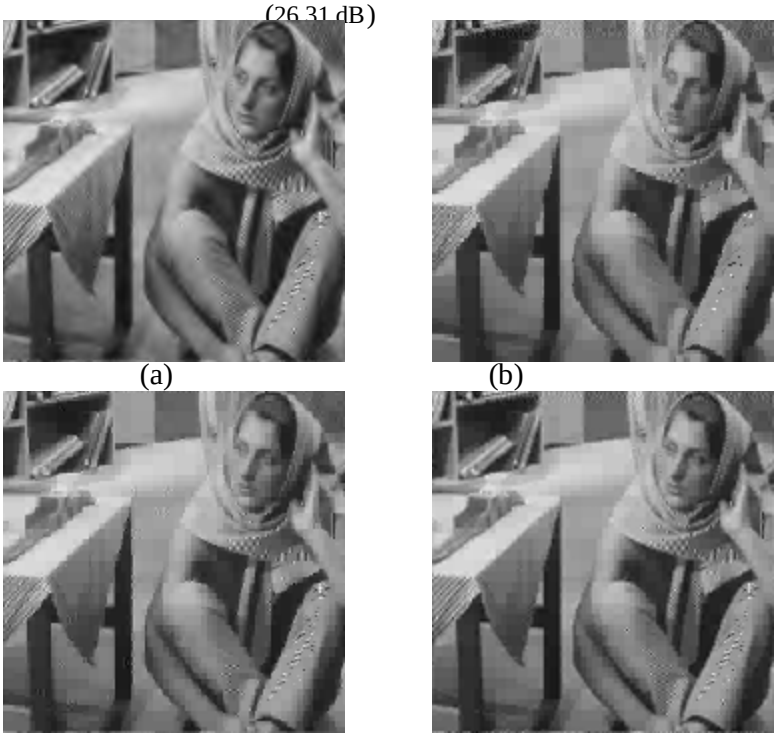

(a) (b)

Figure (6) The restored version of the image «Barbara», compressed to 0.125 bpp using two-dimensional algorithm MECT bit wavelet-based structures :

a – B_F^9 **(23.76 dB); b –** H_F^9 **(22.58 dB); c–** $B_F^1 H_F^8$ **(22.90 dB);d –** $B_F^2 H_F^7$ **(23.29 dB); e –** $B_F^3 H_F^6$ **(23.54 dB); f –** $B_F^4 H_F^5$ **(23.50 dB);g –** $B_F^5 H_F^4$ **(23.75 dB); h –** $H_F^1 B_F^3 H_F^5$ **(23.57 dB)**